

A model-based framework to optimize pharmaceuticals freeze drying

Original

A model-based framework to optimize pharmaceuticals freeze drying / Fissore, Davide; Pisano, Roberto; Barresi, Antonello. - In: DRYING TECHNOLOGY. - ISSN 0737-3937. - STAMPA. - 30:9(2012), pp. 946-958.
[10.1080/07373937.2012.662711]

Availability:

This version is available at: 11583/2485257 since:

Publisher:

TAYLOR & FRANCIS INC

Published

DOI:10.1080/07373937.2012.662711

Terms of use:

This article is made available under terms and conditions as specified in the corresponding bibliographic description in the repository

Publisher copyright

(Article begins on next page)

This is an Accepted Manuscript of an article published by Taylor & Francis Group in *Drying Technology* on 24/05/2012 (Volume 30, Issue 9, pages 946-958, 2012), available online: <http://www.tandfonline.com/doi/abs/10.1080/07373937.2012.662711>.

A model-based framework to optimize pharmaceuticals freeze-drying

Davide Fissore, Roberto Pisano, Antonello A. Barresi

*Dipartimento di Scienza dei Materiali e Ingegneria Chimica,
Politecnico di Torino, corso Duca degli Abruzzi 24, 10129 Torino (Italy)*

Abstract

This paper is focused on the design of pharmaceuticals freeze-drying recipes using in-line or off-line tools. In particular, the Model Predictive Control system is here used to optimize in-line the process, while the design space is used for the off-line optimization. As both methods uses a mathematical model of the process, the problem of estimating the model parameters, including their uncertainty or variability in the lot of vials, is addressed. Then, the strengths and the weaknesses of the various methods are discussed, with particular emphasis on their robustness and their application in industrial-scale freeze-dryers. In particular, the ability of the Model Predictive Control tool to get the optimal recipe in only one run, and its capacity to manage the system in case of an in-line modification of the product properties are shown. For this purpose, experimental results obtained for sucrose and mannitol-based formulations are presented.

Key words

Design space, mannitol, mass transfer resistance, mathematical modeling, Model Predictive Control, sucrose, Process Analytical Technology

Introduction

Freeze-drying is a process generally used to recover an active pharmaceutical ingredient, that, in most cases, is a heat-sensitive molecule, from a solution (commonly an aqueous one). At first product temperature is lowered, thus freezing most of the water of the solution (the “free” water), and, then, the surrounding pressure is lowered, thus causing ice sublimation (primary drying); during this step heat must be supplied to the product, as the ice sublimation is endothermic. Finally, a desorption step (secondary drying) is required to remove the water adsorbed to the product (the “bound” water): this is achieved by increasing product temperature.

Various vials containing the liquid product are placed over the shelves of the freeze-dryer: the operating conditions, i.e. the temperature of the shelves and the pressure in the drying chamber, have to be carefully selected in order to preserve product quality. This result is achieved if product temperature is maintained below a limit value (corresponding to the glass transition value for an amorphous product, or to the melting temperature for a crystalline product) throughout the drying steps. With this respect, primary drying is the most risky phase of the whole process, due to the higher water content of the drying cake. In addition, it must be considered that a reduction of the drying temperature strongly increases the drying time, therefore the process should be carried out not far from the maximum allowable temperature.^[1]

A further constraint is posed by the equipment, as the sublimation flux should be lower than a limit value that would cause choked flow in the duct connecting the drying chamber to the condenser.

The design of the freeze-drying recipe, i.e. the identification of the optimal values of shelf temperature, chamber pressure, and process duration, is generally obtained by means of an extended experimental investigation: this approach is time consuming, expensive, and it does not guarantee that the optimal solution is obtained. With this regard, the design of experiments (DOE) is an effective tool to define an experimentation strategy that minimizes the use of resources maximizing the learning. Moreover, further experiments are generally required to adapt the recipe for the industrial scale apparatus; the scale-up is still one of the major problems.^[2, 3] In addition, it must be said that product and process design are refined as the product goes ahead through stages of development and clinical studies. Therefore, to bring a product to market, scale-up and transfer technology can occur multiple times.^[4]

After the issue of the Guidance for Industry PAT by US-FDA in 2004 various methods

were proposed and tested to design in-line the recipe, thus avoiding testing final product quality, namely:

- i) Expert systems, like the SMARTTM Freeze-Dryer^[5,6];
- ii) Control systems that allow optimizing in-line the process, like LyoDriver^[7,8] or Model Predictive Control (MPC) algorithms^[9,10] wherein the system state is regularly updated (e.g. by the pressure rise test technique), or like that proposed by Fissore et al.^[11] that is based on an almost continuous estimation of the system state.

Both systems presents the same advantages:

- They provide the optimal recipe (according to the target specified) in just one test;
- They can be used in principle both in lab-scale and in large-scale freeze-dryers, thus avoiding the necessity to scale-up the recipe.

The main drawbacks are the followings:

- They require a device to monitor the state of the product (the temperature and the residual amount of ice), as well as to estimate in-line one or more parameters of the model used to calculate the control actions;
- Even if it can be introduced a safety margin on the maximum value of the product temperature, they do not provide any information about the robustness of the recipe in case of process transfer.

As an alternative, it is possible to optimize off-line the recipe using a mathematical model of the process to build the Design Space of the formulation^[12-15], i.e. the range of the operating variables that guarantee to obtain a product with acceptable quality. The use of a mathematical model allows calculating the design space very quickly, but to be effective the model has to be accurate and involve few parameters that can be easily estimated by a limited number of experiments. As an alternative, the determination of the design space can also rely on the statistical design of experiments or better, to reduce the effort required, on a combination of Design of Experiments (DOE) and mathematical modeling as proposed by Sundaram et al.^[15]; these authors also showed how a mathematical model of the equipment can be effectively used to modify in-line a recipe in case of a manufacturing deviation (such as a sharp variation in chamber pressure). The design space approach offers different advantages with respect to the in-line optimization:

- It gives a detailed “picture” of the system, showing the effect of the operating conditions on product temperature and sublimation flux;
- It is possible to get information about the robustness of the recipe, i.e. the effect of

variations in processing conditions on the temperature of the product and, in turn, on its quality;

but also some drawbacks:

- It is necessary a preliminary investigation to determine
- the model parameters, and this investigation has to be carried out both in the lab-scale and in the industrial-scale freeze-dryer;
- As the parameters uncertainty has to be taken into account when building the design space, the recipe can be too conservative.

This paper aims to compare various model-based techniques that have been recently proposed to optimize the primary drying of a vial freeze-drying process, with particular emphasis on their robustness and their application in industrial-scale freeze-dryers. Results obtained when designing a recipe using either an in-line control system or the design space of the process, will be used to point out the strengths and the weaknesses of the various methods.

Methods and Materials

Process model

Mathematical modeling can be very useful to design the recipe of a pharmaceuticals freeze-drying process, but only if the proper model is selected, taking into account the complexity of the process, as well as the parameters that must be determined. Detailed and accurate models can be found in the literature (a review of the various models is given, among the others, in Ref.^[16]), but the level of detail must be chosen according to the final use. It must be stressed that the quality of the prediction generally depends more on the uncertainty connected with the parameters used, than on the complexity (and the dimension) of the model. The good engineering rule is that the model must be the simplest one that gives accurate results. Moreover, the time required for process simulation should be short, in particular when the model is used for an in-line optimization. In the followings we will use one of the simplified models proposed and validated by Velardi and Barresi^[16]: it is a one-dimensional model, where the radial gradients of temperature and composition are neglected, and the heat flux to the product and the sublimation flux of the solvent are calculated using the following equations:

$$J_q = K_v (T_{\text{fluid}} - T_B) \quad (1)$$

$$J_w = \frac{1}{R_p} (P_{w,i} - P_{w,c}) \quad (2)$$

The heat flux is assumed to be proportional to the difference between the temperature of the heating fluid and the temperature of the product at the vial bottom. Actually, the vials can be heated also by radiation, from the chamber walls and the upper shelf, and by conduction from metal frames, when they are used to load the batch. Thus, the coefficient K_v has to be considered as an overall effective heat transfer coefficient, whose value can be different depending on the relative contribution of the various heat transfer mechanisms, which vary with respect to the position of the vial in the batch. The heat transfer coefficient is a function also of the types of vial and equipment used, and of chamber pressure. The heat transfer between the heating fluid and the product at the bottom of the vial can be described as a set of resistors in series, whose overall resistance is the sum of the individual resistances.^[17] Generally, a non-linear equation is used to take into account the dependence of K_v on P_c , as shown in eq. (3):

$$K_v = \left(\left(C_1 + \frac{C_2 P_c}{1 + C_3 P_c} \right)^{-1} + \frac{s_{\text{glass}}}{\lambda_{\text{glass}}} + \frac{1}{k_s} \right)^{-1} \quad (3)$$

The solvent flux is assumed to be proportional to the driving force given by the difference between the vapor pressure at the interface of sublimation and the water partial pressure in the drying chamber^[18], which is generally assumed to be equal to the total chamber pressure. The water partial pressure at the interface is a well known function of T_i : we used the equation proposed by Goff and Gratch^[19], whose results are in good agreement with data reported by Wagner et al.^[20] and with experimental data reported by Marti and Mauersberger.^[21]

In this work, it is convenient to express the vapor flow rate in eq. (2) in terms of R_p , instead of the effective diffusivity coefficient as done by Velardi and Barresi^[16], which can be derived from the dusty gas model.^[22] In fact, the parameter R_p is the total resistance to the vapor flow, and includes the contribution of the dried layer, the stopper, and the chamber; instead, the effective diffusivity coefficient can take into account only the contribution of the cake, and it can be effectively used only if the structure of the porous matrix is uniform. However, it is possible to pass from one notation to the other using the following relationship:

$$\frac{1}{R_p} = \frac{1}{R_{p,1}} + \frac{1}{R_{p,2}} = \frac{k_1 M_w}{RT_i L_{\text{dried}}} + \frac{1}{R_{p,2}} \quad (4)$$

where $R_{p,1}$ is the resistance to the mass transfer due to the dried product, while $R_{p,2}$ takes into account all the other contributions (chamber, stopper, etc..).

The parameter R_p is a function of the formulation investigated, the nucleation temperature, the stopper, and the dried layer thickness.^[23] This last dependence can be expressed according to the following equation:

$$R_p = R_{p,0} + \frac{P_1 L_{\text{dried}}}{1 + P_2 L_{\text{dried}}} \quad (5)$$

Even if the apparatus characteristics are the same, the value of $R_{p,0}$ (i.e. R_p at $L_{\text{dried}} = 0$) can vary with the type of formulation, as it also takes into account the structure of the product at the top surface, and this contribution can be different. For example, sucrose-based formulations tend to form a very compact layer at the top surface of the cake, which is responsible of a high value of $R_{p,0}$. On the contrary, mannitol-based formulations are usually characterized by an open structure at the top surface, which offers a lower value of $R_{p,0}$.

At the interface of sublimation there is no heat accumulation, therefore all the heat flux is used for ice sublimation, and the following equation can be written^[16]:

$$\left(\frac{1}{K_v} + \frac{L_{\text{frozen}}}{\lambda_{\text{frozen}}} \right)^{-1} (T_{\text{fluid}} - T_i) = \Delta H_s \frac{1}{R_p} (P_{w,i} - P_{w,c}) \quad (6)$$

where λ_{frozen} is the effective thermal conductivity of the frozen product, which takes into account the contribution of both the ice and the product. The following equation gives product temperature at the vial bottom:

$$T_B = T_{\text{fluid}} - \frac{1}{K_v} \left(\frac{1}{K_v} + \frac{L_{\text{frozen}}}{\lambda_{\text{frozen}}} \right)^{-1} (T_{\text{fluid}} - T_i) \quad (7)$$

Finally, the evolution of frozen product thickness is calculated by solving eq. (8):

$$\frac{dL_{\text{frozen}}}{dt} = - \frac{1}{\rho_{\text{frozen}} - \rho_{\text{dried}}} \frac{1}{R_p} (P_{w,i} - P_{w,c}) \quad (8)$$

Determination of model parameters

In order to solve the equations of the freeze-drying model previously described we need to know the value of two parameters, namely K_v and R_p , beside the operating conditions (T_{fluid} and P_c) and some physical parameters (ρ_{frozen} , ρ_{dried} , k_{frozen} , ΔH_s).

The value of the overall effective heat transfer coefficient can be calculated if the coefficients C_1 , C_2 , and C_3 are known. Various expressions were provided in the past to this purpose, but reliable values can be obtained only from experimental investigation.^[17, 18, 24]

The following methods were proposed in the literature:

- Gravimetric test;

- Tunable Diode Laser Absorption Spectroscopy (TDLAS): it is used to determine the sublimation flux J_w and, in case T_B is measured, the value of K_v can be calculated as^[25-27]:

$$K_v = \frac{J_w \Delta H_s}{\frac{1}{\Delta t} \int_0^{\Delta t} (T_{\text{fluid}} - T_B) dt} \quad (9)$$

- One of the algorithms proposed to monitor the process using the pressure rise test (PRT): the valve in the duct connecting the drying chamber to the condenser is closed for a short time interval, and the state of the product (temperature and residual ice content), as well as some model parameters (e.g. K_v) are determined looking for the best fit between the measured and the calculated values of pressure rise.^[28-33]

We propose to use the gravimetric test to determine the value of K_v as this test is able to provide the distribution of the values of this parameters among the vials of the batch (both the TDLAS method and the PRT-based methods estimate only a “mean” value of the overall heat transfer coefficient, assumed to be the same for all the vials of the batch) and it can be carried out both in lab-scale and in industrial-scale freeze-dryers. With this respect, the use of wireless temperature sensors appears to be able to solve the problem related to the use of wired thermocouples in industrial freeze-dryers with automatic vial loading/unloading systems.^[34-35] It has to be remarked that at least three different tests, each of them carried out at a different value of chamber pressure, are required in order to estimate the coefficients C_1 , C_2 , and C_3 looking for the best fit between the measured values of K_v and those calculated using eq. (3).

With respect to the resistance of the dried layer to vapor flow, this parameter can be determined using one of the following methods:

- TDLAS: the measurement of the flux of solvent can be used to calculate R_p in case T_i is known, and using the following equation:

$$R_p = \frac{P_{w,i} - P_{w,c}}{J_w} \quad (10)$$

- One of the algorithms used to interpret the PRT;
- The “capillary tube” model proposed by Rambhatla et al.^[36]: it correlates the BET specific surface area of the product to the value of R_p ;
- A weighing device (i.e. Lyobalance) in the drying chamber: if product temperature in the weighed vials is measured, then eq. (10) can be used to get R_p (the sublimation flux is easily obtained from the measurement of the weight loss).^[37]

In-line optimization: Model Predictive Control algorithm

A Model Predictive Control (MPC) algorithm calculates a sequence of control actions, one for each sampling interval, solving an optimization problem with a quadratic objective function:

$$\min_{u(k)} (F_1) = \min_{u(k)} \left\{ \sum_{j=k+1}^{k+h_p} \left[y_{\text{ref}}(j) - (y(j) + \hat{e}(k)) \right]^2 \right\} \quad (11)$$

In eq. (11) y_{ref} is the assigned set-point for the output variable y at the time instant j , and h_p is the prediction horizon, i.e. the number of time intervals in the future where the state of the system is predicted, given the initial state and the sequence of control actions. The value of the manipulated variable u is assumed to remain constant throughout the sampling interval (t_k, t_{k+1}). After each sampling time the modeling error e can be calculated as the difference between the measured and the calculated values of the output variable as shown in the following:

$$e_k = \tilde{y}_k - y_k \quad (12)$$

As the correction e may be due to modeling errors or measurement noise (or error), a simple filter can be used to make this value less sensitive to measurement noise, e.g. we can use the following equation:

$$\hat{e}_k = \alpha e_k + (1 - \alpha) e_{k-1} \quad (13)$$

where α , called forgetting factor, is equal to 0 in case only measurement errors are responsible for e , or it is equal to 1 in case there are no noises to filter. Once the new estimation of \hat{e}_k is available, the optimization problem is solved again for the following time interval.

In eq. (11) it is possible to take into account the cost of the control actions. In case there are n_c manipulated variables, the optimization problem solved by the MPC algorithm is the following^[8]:

$$\min_{u(k) \dots u(k+h_c-1)} \left\{ \sum_{j=k+1}^{k+h_p} \left[y_{\text{ref}}(j) - (y(j) + \hat{e}(k)) \right]^2 + \sum_{r=1}^{n_c} w_{u,r} \sum_{j=k+1}^{k+h_c-1} \left[u_r(j) - u_r(j-1) \right]^2 \right\} \quad (14)$$

thus looking for a sequence of control actions u that minimize not only the offset of the controlled variables with respect to the target values, but also the variations of the manipulated variables. $w_{u,r}$ is the move suppression factor, a parameter used to weigh the contribution of the variation of the r -th manipulated variable to the cost function. h_c is the control horizon, i.e. the number of time intervals in the future where the value of the manipulated variables is calculated (h_p may be larger than h_c ; in this situation for the time

instant between h_c and h_p the manipulated variables assume the values they have in the final instant of the control horizon).

The manipulated variables in a freeze-drying process are T_{fluid} and P_c . Two different cases can be considered:

- i. Both T_{fluid} and P_c are manipulated;
- ii. Only T_{fluid} is manipulated.

With respect to the target of the operation, we need to minimize the duration of the drying time, that depends on the sublimation flux. Thus, in case (i) the controller will minimize the difference between the sublimation flux and a target value (e.g. the maximum value allowed in the apparatus considered), while in case (ii) the controller will minimize the difference between maximum product temperature and the limit value: in fact, when P_c is not modified, the sublimation flux is maximized if the product is maintained at the maximum allowed temperature.

Various constraints can be taken into account when solving the quadratic problem (eq. (14)), namely:

- i. product temperature has to be maintained below the maximum allowed value;
- ii. the sublimation flux has to remain below a limit value that is a characteristic of the equipment;
- iii. minimum and maximum values of T_{fluid} , P_c and heating and cooling rates that can be obtained in the apparatus.

These constraints are handled in the optimization problem through proper penalty functions, one for each variable, that are added to the cost function in eq. (14). To predict the future evolution of the controlled variable y (i.e. J_w or T_B), the MPC system uses the mathematical model of the process above described, which is also used in the following for the off-line optimization. Further details about the algorithm can be found in Pisano et al. ^[10], who also investigated the robustness of the control system. With this regard, they showed that the system can effectively control the temperature of the product even when the mathematical model of the process does not perfectly describe the real dynamics of the process, e.g. because of the uncertainty on the parameters of the model (K_v and R_p). In addition, it can reject any disturbance that can modify the performances of the equipment, relying on the receding horizon policy to adjust the recipe according to a new estimation of the product state that is provided by the monitoring system. Nevertheless, it must be said that the robustness of the control system does not guarantee that the resulting recipe is robust. In fact, if such a recipe is used (without any modifications, but using the fixed sequence of set-point values previously

determined) to carry out a new freeze-drying cycle in the same equipment, or worse in a new freeze-dryer, even small variations in the processing conditions might infringe the constraint on the product temperature. A simple, but effective, way to overcome such a problem is introducing a safety margin on the maximum value of T_B ; this margin is here indicated as χ_{T_B} . By this way, the optimal heating policy calculated by the MPC system can maintain the temperature of the product close, but always below, $(T_B - \chi_{T_B})$. Such a recipe can withstand all those variations in processing conditions, or in process parameters, that results in temperature increases lower than χ_{T_B} . Of course, the value of χ_{T_B} required to get a robust recipe depends on the range of variations of T_{fluid} and P_c , or K_v and R_p , considered: in fact the value of χ_{T_B} increases with the range of variability considered. To evaluate the impact of the chosen disturbances on the maximum value of T_B and thus of χ_{T_B} , we can use the same mathematical model at the basis of MPC calculations.

Off-line optimization: Design Space

The design space can be calculated using the method proposed by Fissore et al.^[14] as it takes into account the variation of the design space with time, due to the increase of the dried layer thickness. Beside T_{fluid} and P_c , the thickness of the dried layer is used as third coordinate of the diagram instead of time, as it allows obtaining a unique diagram for the formulation considered. The procedure used to build the design space is the following:

1. Identification of the values of T_{fluid} and P_c of interest. The third parameter, L_{dried} , ranges from 0 to 1, and it is required to set a sampling interval also for this variable.
2. Selection of the first value of L_{dried} to be considered in the design space.
3. Selection of a couple of values of T_{fluid} and P_c and calculation of product temperature (T_i and T_B) and sublimation flux (J_w) when the operating conditions are set equal to the selected values. The temperature T can be calculated from eq. (6), and the sublimation flux is obtained from eq. (2), once T_i has been determined.
4. For the selected value of L_{dried} , the operating conditions T_{fluid} and P_c belong to the design space in case both maximum product temperature is lower than the limit value, and the sublimation flux is lower than the maximum allowed value.
5. Repetition of previous calculations for all the operating conditions of interest, thus obtaining the full design space for the value of L_{dried} previously considered.

6. Repetition of previous calculations for the other values of L_{dried} of interest, thus determining how the design space changes during the primary drying.

The effect of parameter uncertainty on the design space of the primary drying can be taken into account using the approach proposed by Giordano et al. [12]

As already discussed for the in-line optimization, also in this case the resulting recipe has to be sufficiently robust to guarantee the quality of the product even in presence of limited variations in processing conditions with respect to the set-point values, or in case the same recipe is used in a different apparatus. Unlike the off-line optimization, a safety margin for the temperature of the heating fluid ($\chi_{T_{\text{fluid}}}$) and for chamber pressure (χ_{P_c}) can be directly introduced during the design of the recipe. An example of how to use the design space to define a recipe that is robust enough to preserve the product even in presence of temperature and pressure oscillations (respectively of amplitude $\chi_{T_{\text{fluid}}}$ and χ_{P_c}) is given in the following section. As an alternative and similarly to what already shown for the in-line optimization, we can introduce a safety margin on the temperature of the product (χ_{T_B}) and calculate a new design space using as target temperature the value $(T_{\text{max}} - \chi_{T_B})$.

Independently of the approach used, it must be said that the robustness of a recipe is not guaranteed if it is transferred to a new equipment, but a new recipe has to be re-calculated according to the design space of the new freeze-dryer and introducing an appropriate safety margin either on the processing conditions or on the maximum allowed product temperature.

Case study

The case study that will be investigated in the following is the freeze-drying of a placebo constituted by a 5% w/w sucrose (Sigma-Aldrich) aqueous solution. The freeze-drying of a 5% w/w mannitol (Riedel de Haën) solution will also be investigated as an example of crystalline product. All reagents were analytical grade and used as received. Solutions were prepared using ultra-pure water (Milli-Q RG, Millipore, Billerica, MA) and processed into ISO 8362-1 2R tubing vials, filled with 1.5 mL of solution.

The process is carried out in a pilot-scale freeze-dryer (LyoBeta 25 by Telstar, Spain) with a chamber volume of 0.2 m³ and equipped with capacitance (Baratron type 626A, by MKS Instruments, Andover, MA, USA) and thermal conductivity (Pirani type PSG-101-S, by Inficon, Bad Ragaz, Switzerland) gauges. The pressure in the drying chamber is regulated by bleeding of inert gas, whose flow rate is measured through a mass flow meter (type MB100,

by MKS Instruments, Andover, MA, USA).

The temperature of the product at the vial bottom is monitored using T-type miniature thermocouples (by Tersid S.p.A., Milano, Italy) placed in both central and edge vials. Instead, the temperature of the product at the interface of sublimation and the residual ice content are estimated using the pressure rise test: the valve placed in the spool connecting the drying and condenser chamber is closed for a short time, and the pressure inside the drying chamber increases because of vapor accumulation. The chamber pressure data are then related to the process parameters of interest using mathematical models. For this purpose, it is here used the DPE⁺ algorithm.^[32]

The end of primary drying is here estimated using the ratio between the pressure measured by Pirani gauge and that supplied by Baratron manometer.^[38] The Pirani gauge is a thermal conductivity sensor, thus its signal depends on the gas type or, in case of a mixture, on the composition. Instead, the Baratron sensor is a capacitance manometer, thus its reading is independent of the gas composition. During the drying, all the gas in the chamber is water vapor, therefore the value of chamber pressure measured by Pirani (that is generally calibrated for nitrogen) is higher than that read by the capacitance manometer. On the contrary, at the end of the drying, when the concentration of water into the drying chamber is very low, the pressure measured by Pirani approaches the value measured by Baratron. Therefore, the completion of ice sublimation can be detected as the time at which the ratio of the pressure signals given by the two gauges approaches unity.^[39]

The heat transfer coefficient is measured by gravimetric way. In particular, a batch of vials is filled with water (or with the solution containing the active pharmaceutical ingredient), weighed and loaded in the drying chamber. After freezing, the primary drying is carried out for a time interval (Δt); then vials are unloaded and weighed. In this manner, the weight loss (Δm) can be easily measured in each vial of the lot. If temperature of the ice at the vial bottom (T_B) is also measured, the coefficient K_v can be calculated using the following equation:

$$K_v = \frac{\Delta m \cdot \Delta H_s}{A_v \cdot \int_0^{\Delta t} (T_{\text{fluid}} - T_B) dt} \quad (15)$$

To estimate the pressure dependence of K_v , such a test has to be repeated at different values of P_c .

Results and discussion

Model Parameters

The type and contribution of the various mechanisms that can be involved in the heat transfer from the technical fluid to the product vary with the position of the vial into the lot. In particular, in case vials are loaded directly on the heating shelf, arranged in clusters of hexagonal arrays and surrounded by a metal band, four groups of vials can be identified^[17]: vials V_1 are located at the edge of the lot and in contact with the metal frame, V_2 are at the edge but not in contact with the band, V_3 are in the second row, and vials V_4 are in the central part of the lot. Nevertheless, for the sake of clarity, in the following analysis we will consider only two groups of vials, which are characterized respectively by the highest (type V_1) and the lowest (type V_4) value of K_v .

The value of K_v vs. P_c for the two groups of vials above cited has been already measured by Pisano et al.^[17] and, according to eq. (3), has been described by a non-linear function whose parameters (C_1 , C_2 and C_3) have been obtained by regression of experimental data (see Table 1). Furthermore, to simplify the design procedure, we assume that the parameter C_1 is the only responsible for the uncertainty on K_v , while the contribution of C_2 and C_3 is implicitly included in the uncertainty of the former parameter. This uncertainty in turn corresponds to the standard deviation of the distribution curve of C_1 (see Table 1), which can be easily derived from the distributions of K_v experimentally observed for the two groups of vials considered.

The value of R_p vs. L_{dried} , for the two formulations considered in this study, was estimated by both Lyobalance and the pressure rise test technique evidencing a good agreement between the two methods, see Figure 1. According to Ref.^[14], the freeze-drying of sucrose-based formulations produces porous materials with an uneven structure, wherein a compact layer at the top surface of the product is present and responsible of the initial, and sharp, increase of R_p . By contrast, mannitol-based formulations are characterized by an open structure at the upper surface and, thus, the value of R_p increases almost linearly with L_{dried} . However, it must be noticed that the resistance to vapor flow observed for 5% w/w mannitol is much higher than that observed for 5% sucrose, and in particular its initial value is approximately equal to the value of R_p observed, for the sucrose-based formulation, after the initial ramp. This behavior might be due a much more irregular structure of the mannitol cake that, even if it is characterized by an open structure at the top surface, offers a higher resistance to vapor flow. Furthermore, we have observed that during the drying step, the couple of temperature and vapor flow increase promotes the formation of numerous holes on

the top surface, which lower the value of R_p .

The parameters of eq. (5), which describe the non-linear dependence of R_p on L_{dried} , have been obtained by regression of experimental data and are reported in Table 2. The uncertainty on the parameter R_p is defined by the accuracy of the temperature sensor used in the experiments. Since the miniature thermocouples used in this study have an accuracy of 0.5 K, the maximum variation in the resistance to mass transfer is about 10% and, in particular, we assume that the only responsible for this uncertainty is the parameter P_1 , as it strongly affects both the final value and the shape of the curve R_p vs. L_{dried} .

Off-line optimization

Following on from what stated in the previous section, the first step to build the design space is the selection of the range of interest for T_{fluid} and P_c , that are respectively (240, 300) K and (2.5, 20) Pa, as well as of the parameters of the model that describe the heat and mass transfer in the investigated system. In particular, the pressure dependence of K_v and the value of R_p vs. L_{dried} are respectively described by eq. (3) and (5), using the coefficients of Table 1 and 2. Therefore, the last parameter to be defined remains the limit value for the temperature of the product (T_{max}). In case of amorphous products like the sucrose-based formulation, the value of T_{max} is set a couple of degrees higher than the glass transition temperature, that is 240 K. On the contrary, in case of crystalline products like the mannitol-based formulation, T_{max} corresponds to the melting temperature, that is 248 K.

As widely discussed by Ref.^[14], the design space usually becomes smaller and smaller as the drying goes on; in fact, the resistance to mass transfer increases with L_{dried} , therefore the range of processing conditions that can be effectively used reduces as ice sublimation proceeds. It follows that to always respect the constraint on the maximum product temperature, the operating conditions have to be changed during the primary drying according to the modifications of the design space or, as it will be done in the following, have to be chosen according to the most restrictive design space, that is, the one calculated close to the completion of ice sublimation when the value of R_p is the highest.

Figure 2 shows an example of design space calculated close to the end of the drying (i.e. at $L_{\text{dried}}/L = 99\%$) for the two selected formulations in case they are processed in edge (V_1) and central vials (V_4). As already shown in the previous section, central vials have a lower value of K_v with respect to those placed at the edge of the shelf and, therefore, the design space is larger. However, if the primary objective is the selection of a combination of T_{fluid} and P_c that guarantees that all the vials of the lot meet product quality requirements, we have

to use the design space of vials V_1 as they might be more easily damaged by product overheating.

Once the design space is built for the selected product, processing conditions that provides assurance of quality can be easily identified. In particular, to determine the optimal combination of T_{fluid} and P_c that maximizes the sublimation flux, we used the contour plot of J_w calculated close to the end of the drying. According to Figure 2 a good combination of processing conditions that preserves the quality of the product for all the vials of the lot, and maximizes the mass flux of vapor, is: (case #1, 5% w/w sucrose) $T_{\text{fluid}} = 255$ K and $P_c = 5$ Pa, and (case #2, 5% w/w mannitol) $T_{\text{fluid}} = 252$ K and $P_c = 5$ Pa. At this point, two freeze-drying cycles were carried out using the constant values of T_{fluid} and P_c selected from the above optimization procedure. The two cycles were then analyzed in terms of product temperature response and duration of the sublimation phase.

The temperature of the product at the vial bottom was monitored by the pressure rise test technique (coupled with DPE⁺ algorithm^[32]) and through thermocouples placed in both central and edge vials. Concerning the product temperature, it must be said that vials hosting thermocouples finish sublimating earlier than the rest of the lot, as the insertion of the sensor probe alters the drying kinetics of the monitored vial. Therefore, thermocouples signals can be considered representative of the system state until ice sublimation is not completed in the monitored vial: such a phenomenon can be easily detected as a sharp increase in the temperature of the product.^[38] The completion of ice sublimation of the rest of the lot was, instead, associated to the beginning of the decreasing part of the Pirani-Baratron pressure ratio curve, when most of the vials of the lot have finished sublimating. An example of results is given in Figure 3, where it can be observed that in both cases the temperature of the product (for both vials V_1 and V_4) remains below T_{max} , and the drying time as measured by Pirani-Baratron pressure ratio resulted to be respectively 27 h for sucrose and 31 h for mannitol.

It must be pointed out that even if the mannitol-based formulation is processed using almost the same value of T_{fluid} and P_c set for the sucrose solution, the resulting sublimation rate is smaller, and therefore the drying time is longer (see Figure 3, graph b). This result is the consequence of a much higher value of R_p vs. L_{dried} observed for the 5% w/w mannitol solution with respect to that observed for the 5% w/w sucrose. In case the product is processed in a different dryer, the two recipes above validated do not guarantee neither that the quality of the final product is respected nor that the heating policy used is not too precautionary, unless the value of K_v vs. P_c , and R_p vs. L_{dried} , is the same in the two pieces of equipment. However, it must be observed that the value of R_p vs. L_{dried} is generally not

modified moving from one equipment to another one, provided that the product undergoes the same freezing conditions in the original and in the new freeze-dryer. On the contrary, the value of K_v of the selected vial can vary with the equipment used (e.g. because of a different surface emissivity), therefore the design space, and the optimal recipe, has to be recalculated according to the value of the heat transfer coefficient observed in the new dryer.

A final comment concerns the robustness of the recipe. Following on from what stated in the introduction, a safety margin can be introduced on both T_{fluid} and P_c to account for deviations from the scheduled values. Depending on the approach used to design the recipe, we can include such margins in different ways, which are better clarified in the following with the aid of an example. Let's consider the freeze-drying of the mannitol-based formulation taking into account that the design space is modified as the drying goes on, see Figure 4. Let's suppose that the objective is the design of a recipe that minimizes the drying time, but preserve the quality of the product even with fluid temperature oscillations of magnitude 5 K. As for 5% w/w mannitol we have observed that the maximum sublimation flux (compatible with product constraints) is achieved at low values of P_c (see Figure 2), let's consider a constant value of chamber pressure ($=5$ Pa) while the temperature of the heating fluid is modified during the drying. To get a recipe that is robust with respect to the process deviation considered, the operating point has to be chosen on the design space in such a way that it is sufficiently close to the curve that represents the limit operating conditions, but at least 5 K below to preserve the quality of the product. An example of such a recipe is displayed in Figure 4 (left-side graphs). The duration of each step has not been here specified, but it can be calculated using the mathematical model of the process as already discussed by Ref. ^[14] In case, instead, the drying is carried out at constant T_{fluid} and P_c , we have that the safety margin on T_{fluid} is not constant over the time, but reduces as the ice sublimation proceeds. Figure 4 (right-side graphs) shows an example of such a single-step recipe wherein the value of T_{fluid} was chosen according to the design space calculated close to the end of the drying, and introducing a safety margin of $\chi_{T_{\text{fluid}}}$ that is at least 5 K. It must be noticed that the recipe designed and validated in this paper (see Figure 2, right-side graphs) have, instead, a margin of safety (at the end of the process) that was 8 K for vials V_4 and less than 1 K for vials V_1 . It follows that this recipe guarantees the quality of the product of central vials (that constitutes almost 80% of the vials of the lot) even in presence of large deviations of T_{fluid} with respect to the set-point value. By contrast, edge-vials can be easily damaged by small variations in T_{fluid} , mainly close to the end of the drying when the margin of safety is smaller. Another possibility

to build a robust recipe consists in using a design space that has been calculated for a lower value of the maximum allowed product temperature (e.g. $= T_{\max} - \chi_{T_B}$). Figure 5 compares the design space of 5% w/w mannitol obtained using different values of χ_{T_B} . As expected, it can be observed that a higher value of χ_{T_B} results in a smaller design space and, therefore, in a more precautionary heating policy and a longer drying time. Figure 5 (upper graph) shows a similar comparison in case a 5% w/w sucrose solution is considered. It must be evidenced that, even if the investigated values of safety margin for sucrose and mannitol-based formulations are the same, the resulting value of the target temperature is different, as the two products have a different value of T_{\max} .

In-line optimization

The minimum values of input variables have been set according to the characteristics of the equipment ($P_{c,\min} = 2.5$ Pa, $T_{\text{fluid},\min} = 193$ K), while their maximum values are $T_{\text{fluid},\max} = 300$ K and $P_{c,\max} = 30$ Pa. The values of model parameters and their dependence on processing conditions and/or product characteristics are described according to eqs. (3) and (5) and the parameters of Table 1 and 2. The parameters of the control system were chosen according to the guidelines given by Ref. ^[10], thus: $h_p = 7$, $h_c = 4$ and $\Delta t_c = 30$ min. The reference trajectory of the controlled variable (that is J_w) was calculated by a local steady-state optimization that takes also into account equipment and product constraints. In particular, the maximum value of J_w , that the system under investigation can manage without incurring in choked flow conditions, is set to $1.5 \text{ kg h}^{-1} \text{ m}^{-2}$. The limit value of the product temperature was, instead, set according to the product characteristics, as already discussed in the previous section. According to Pisano et al.^[10], we have used the same value (i.e. 0.1) for the move suppression factors $w_{u,1}$, that penalizes variations in T_{fluid} , and $w_{u,2}$ that penalizes changes in P_c . At the completion of each control action, the state of the system (in terms of J_w and T_B) is updated using the estimations obtained by the pressure rise test technique coupled with DPE⁺ algorithm. Then, a new set of control actions is calculated starting from the new system state, and taking also into account the error of the model predictions. It must be remarked that the used monitoring technique gives an average estimation of the system state, which however is very close to that of central vials as they constitute about 80% of the lot. It follows that the control system can effectively control the product temperature of only central vials.

Figure 6 compares the control strategies obtained when using the two MPC control

algorithms described above to optimize in-line the recipe in case the 5% w/w sucrose solution is freeze-dried. For the first control system (that manipulates only T_{fluid} : left-side graph), the set pressure value is maintained constant during the entire cycle and equal to 5 Pa, which corresponds to the optimal value calculated by the off-line optimization of the process. In both cases, the controller maximizes the heating in the first half of the drying to lead J_w towards its target value. In the second part of the drying, instead, variations in input variables are much more limited as J_w is already close to the maximum value that can be achieved compatibly with the constraint on product temperature. In addition, it must be remarked that in both cases the temperature of the product in central vials remains always below T_{max} throughout the primary drying phase, thus preserving the quality of the product. A further remarkable reduction of the drying time is obtained when optimizing both T_{fluid} and P_c (from about 27 h of the off-line optimization to 22 h in case of manipulation of only T_{fluid} , and to about 15 h in case both T_{fluid} and P_c can be modified), but it must be said that a much higher difference might be observed in case the process is carried out under mass transfer control, when the manipulation of only T_{fluid} is not sufficient to properly control the temperature of the product. Nevertheless, it must be noticed that in case also P_c is manipulated, the temperature of the product is maintained closer to T_{max} ; in particular, while the mean value of T_B as estimated by the pressure rise test technique is always below its limit value, the temperature of vials V_1 (as measured by thermocouples) overcame T_{max} and thus the quality of their content was not guaranteed. As all the control systems so far proposed in the field of freeze-drying do not take into account inter-vial variability, to guarantee that the entire lot of vials meets product quality requirements we can use two strategies:

1. Use as control variable the product temperature of edge-vials, which might be more easily overheated (of course, this approach requires to estimate, or to measure, this variable, which is not an easy task and implies the use of sophisticated devices as those proposed by Refs. ^[40-43]);
2. Reduce the value of T_{max} by a safety margin (χ_{T_B}), which accounts for the temperature variance of the lot around the mean value that can be, for example, estimated though the pressure rise test technique.^[44]

Following on from what stated in the introduction, the same approach can be used to take into account potential disturbances on processing conditions. Nevertheless, it must be evidenced that such an approach does not guarantee the robustness of the recipe in case it is transferred to a different equipment, unless a very large safety margin on T_{max} is introduced. In this case,

the best solution is to repeat the test on the new equipment.

Finally, it can be observed that the operating conditions set by the control system (in case of manipulation of both T_{fluid} and P_c) do not belong to the design space of central vials reported in Figure 2. This result is the consequence of a significant reduction of the value of R_p vs. L_{dried} that, in turn, is likely due to the cracking of the crust promoted by a much higher value of J_w at the beginning of the drying: in fact, comparing the maximum value of J_w observed in the two tests (see Figure 6, graphs b) the manipulation of P_c allows to reach a value of $J_{w,\text{max}} = 3.2 \times 10^{-4} \text{ kg s}^{-1} \text{ m}^{-2}$ that is significantly higher with respect to the case in which only T_{fluid} is manipulated ($J_{w,\text{max}} = 2.0 \times 10^{-4} \text{ kg s}^{-1} \text{ m}^{-2}$).

A similar study was carried out for the mannitol-based formulation. In this case, the comparison was done only between the in-line (see Figure 3, right-side graphs) and the off-line optimization in case of manipulation of both T_{fluid} and P_c (see Figure 7). Even in this case, the control system could maintain the temperature of the product below its limit value, and shorten the duration of the sublimation phase with respect to the off-line optimization (26 h vs. 31 h). However, in this case (with respect to the sucrose-based formulation) the manipulation of the chamber pressure seems to be less effective in terms of drying time reduction (16% for mannitol vs. 44% for sucrose). Nevertheless, it must be said that the significant reduction of the drying time observed for the freeze-drying of sucrose is partially due to a variation in R_p that further promotes the sublimation of ice. In general, if the structure of the product is not modified, and provided that the value of R_p vs. L_{dried} of 5% w/w mannitol solution is much higher than that of sucrose, the role of chamber pressure would be more marked in case of freeze-drying of mannitol solutions, as in this case mass transfer control conditions might more easily occur.

Conclusion

The effectiveness of various model-based strategies to optimize a freeze-drying process has been demonstrated by means of experimental investigations. The off-line optimization via design space provides much more information about the effect of the operating conditions (T_{fluid} and P_c) on the product, but the recipe optimization can be less effective than that achieved using the model predictive control algorithm. However, to provide an effective in-line optimization, the dryer has to be equipped by a proper monitoring device that, mainly in a manufacturing plant, is not always available.

Both approaches can be used both in small-scale and in large-scale freeze-dryers, thus avoiding the successive step that requires the scale-up of the recipe. However, when using the model predictive control system it is possible to get the optimal recipe in just one run, and potential disturbances affecting the dynamics of the process can be rejected. For example, in this work it has been shown that even in case one of the parameter of the model (i.e. R_p) is significantly modified during the cycle (e.g. because of crust cracking or micro-collapse of the structure), the in-line optimization can effectively manage this situation preserving the quality of the product. By contrast, a similar situation can be successfully managed by the off-line optimization only introducing a large uncertainty on model parameters that, however, lead toward a more precautionary cycle and therefore a longer drying time.

Acknowledgements

The contribution of Giovanni Accardo and Alberto Vallan (Politecnico di Torino) for respectively the experimental investigation and the set-up of the weighing device is gratefully acknowledged.

List of Symbols

A_v	cross sectional area of the vial, m^2
C_1	parameter used in eq. (3), $W K^{-1} m^{-2}$
C_2	parameter used in eq. (3), $W K^{-1} m^{-2} Pa^{-1}$
C_3	parameter used in eq. (3), Pa^{-1}
e	modeling error
\hat{e}	filtered value of the modeling error
F_1, F_2	cost functions to be minimized
ΔH_s	sublimation heat, $J kg^{-1}$
h_c	control horizon
h_p	prediction horizon
J_q	heat flux to the product, $W m^{-2}$
J_w	solvent sublimation flux, $kg m^{-2} s^{-1}$
K_v	overall effective heat transfer coefficient, $W K^{-1} m^{-2}$
k_1	effective diffusivity of water vapor in the dried layer, $m^2 s^{-1}$
k_s	heat transfer coefficient between the technical fluid and the shelf, $W K^{-1} m^{-2}$
L	total product thickness, m
L_{dried}	thickness of the dried layer, m
L_{frozen}	thickness of the frozen layer, m
m	mass, kg
n_c	number of manipulated variables
P_1	parameter used in eq. (5), s^{-1}
P_2	parameter used in eq. (5), m^{-1}
P_c	chamber pressure, Pa
$P_{w,c}$	solvent partial pressure in the drying chamber, Pa
$P_{w,i}$	solvent partial pressure at the sublimation interface, Pa
R	ideal gas constant, $J kmol^{-1} K^{-1}$
R_p	resistance of the dried layer to vapor flux, $m s^{-1}$
$R_{p,0}$	parameter used in eq. (5), $m s^{-1}$
s_{glass}	thickness of the glass at the bottom of the vial, m
T_i	product temperature at the interface of sublimation, K
T_B	product temperature at the bottom of the vial, K
T_{fluid}	temperature of the heating fluid, K

T_{\max}	maximum allowable product temperature, K
t	time, s
Δt_c	control interval, min
u	manipulated variable
w_u	move suppression factor
y	controlled variable
\tilde{y}	measured value of the controlled variable
y_{ref}	set-point for the controlled variable

Greeks

α	forgetting factor
χ	safety margin
ρ_{frozen}	density of the frozen product, kg m^{-3}
ρ_{dried}	apparent density of the dried product, kg m^{-3}
λ_{frozen}	heat conductivity of frozen product, $\text{W m}^{-1}\text{K}^{-1}$
λ_{glass}	heat conductivity of the glass, $\text{J s}^{-1}\text{m}^{-1}\text{K}^{-1}$

Abbreviations

DPE	Dynamic Parameters Estimation
MPC	Model Predictive Control
PAT	Process Analytical Technology
PRT	Pressure Rise Test
TDLAS	Tunable Diode Laser Absorption Spectroscopy

References

- 1 Barresi, A.A., Ghio, S.; Fissore, D.; Pisano, R. Freeze drying of pharmaceutical excipients close to collapse temperature: influence of the process conditions on process time and product quality. *Drying Technology* **2009**, *27*, 805-816.
- 2 Barresi, A.A. Overcoming common lyophilization scale-up issues. *Pharmaceutical Technology Europe* **2011**, *23*, 29. The complete electronic version is available at <http://www.pharmtech.com/barresi>
- 3 Fissore, D.; Barresi, A.A. Scale-up and process transfer of freeze-drying recipes. *Drying Technology* **2009**, *29*, 1673-1684.
- 4 Trappler, H.E. Freeze drying, scale-up considerations. In *Encyclopedia of Pharmaceutical Technology*; Swarbrick, J., Ed.; Informa Healthcare: New York, 2006; 1834-1849.
- 5 Tang, X.C.; Nail, S.L.; Pikal, M.J. Freeze-drying process design by manometric temperature measurement: Design of a smart freeze-dryer. *Pharmaceutical Research* **2005**, *22*, 685-700.
- 6 Gieseler, H.; Kramer, T.; Pikal, M.J. Use of manometric temperature measurement (MTM) and SMART™ freeze dryer technology for development of an optimized freeze-drying cycle. *Journal of Pharmaceutical Sciences* **2007**, *96*, 3402–3418.
- 7 Fissore, D.; Pisano, R.; Velardi, S.A.; Barresi, A.A.; Galan M. PAT tools for the optimization of the freeze-drying process. *Pharmaceutical Engineering* **2010**, *29*, 58-70.
- 8 Pisano, R.; Fissore, D.; Velardi, S.A.; Barresi A.A. In-line optimization and control of an industrial freeze-drying process for pharmaceuticals. *Journal of Pharmaceutical Sciences* **2010**, *99*, 4691-4709.
- 9 Daraoui, N.; Dufour, P.; Hammouri, H.; Hottot A. Model predictive control during the primary drying stage of lyophilisation. *Control Engineering Practice* **2010**, *18*, 483-494.
- 10 Pisano, R.; Fissore, D.; Barresi, A.A. Freeze-drying cycle optimization using Model Predictive Control techniques. *Industrial Engineering Chemistry Research* **2011**, *50*, 7363-7379.
- 11 Fissore, D.; Velardi, S.A; Barresi, A.A. In-line control of a freeze-drying process in vial. *Drying Technology* **2008**, *26*, 685-694.
- 12 Giordano, A.; Barresi, A.A.; Fissore, D. On the use of mathematical models to build the design space for the primary drying phase of a pharmaceutical lyophilization process. *Journal of Pharmaceutical Sciences* **2011**, *100*, 311-324.
- 13 Koganti, V.R.; Shalaev, E.Y.; Berry, M.R.; Osterberg, T.; Youssef, M.; Hiebert, D.N.;

Kanka, F.A.; Nolan, M.; Barrett, R.; Scalzo, G.; Fitzpatrick, G.; Fitzgibbon, N.; Luthra, S.; Zhang, L. Investigation of design space for freeze-drying: use of modeling for primary drying segment of a freeze-drying cycle. *AAPS PharmSciTech* **2011**, *12*, 854-861.

14 Fissore, D.; Pisano, R.; Barresi, A.A. Advanced approach to build the design space for the primary drying of a pharmaceutical freeze-drying process. *Journal of Pharmaceutical Sciences* **2011**, *100*, 4922-4933.

15 Sundaram, J.; Hsu, C.C.; Shay, Y.M.; Sane, S.U. Design space development for lyophilization using DOE and process modeling. *BioPharm International* **2010**, *23*, 26-36.

16 Velardi, S.A.; Barresi, A.A. Development of simplified models for the freeze-drying process and investigation of the optimal operating conditions. *Chemical Engineering Research and Design* **2008**, *86*, 9-22.

17 Pisano, R.; Fissore, D.; Barresi, A. A.. Heat transfer in freeze-drying apparatus. In: *Heat transfer - Book I*; dos Santos Bernardes M.A., Ed.; InTech - Open Access Publisher: Rijeka, 2011, 91-114.

18 Pikal, M. J. Heat and mass transfer in low pressure gases: applications to freeze-drying. In *Transport Processes in Pharmaceutical Systems*; Amidon, G.L., Lee, P.I., Topp, E.M., Eds.; Marcel Dekker: New York, 2000; 611-686.

19 Goff, J.A.; Gratch, S. Low-pressure properties of water from -160 to 212°F. *Transaction of the American Society of Venting Engineering* **1946**, *52*, 95-122.

20 Wagner, W.; Saul, A.; Pruss, A. International equations for the pressure along the melting and along the sublimation curve of ordinary water substance. *Journal of Physical and Chemical Reference Data* **1994**, *23*, 515-525.

21 Marti, J.; Mauersberger, K. A survey and new measurements of ice vapor pressure at temperatures between 170 and 250 K. *Geophysical Research Letters* **1993**, *20*, 363-366.

22 Kast, W., Hohenthanner, C. R. Mass transfer within the gas phase of porous media. *International Journal of Heat and Mass Transfer* **2000**, *43*, 807-823.

23 Pikal, M.J. Use of laboratory data in freeze drying process design: heat and mass transfer coefficients and the computer simulation of freeze drying. *Journal of Parenteral Science Technology* **1985**, *39*, 115-139.

24 Pikal, M.J.; Roy, M.L.; Shah, S. Mass and heat transfer in vial freeze-drying of pharmaceuticals: role of the vial. *Journal of Pharmaceutical Sciences* **1984**, *73*, 1224-1237.

25 Kessler, W.J.; Davis, S.J.; Mulhall, P.A.; Finson, M.L. System for monitoring a drying process. United States Patent No. 0208191 A1, 2006.

26 Gieseler, H.; Kessler, W.J.; Finson, M.; Davis, S.J.; Mulhall, P.A.; Bons, V.; Debo,

D.J.; Pikal, M.J. Evaluation of Tunable Diode Laser Absorption Spectroscopy for in-process water vapor mass flux measurement during freeze drying. *Journal of Pharmaceutical Sciences* **2007**, *96*, 1776-1793.

27 Kuu, W.Y.; Nail, S.L.; Sacha, G. Rapid determination of vial heat transfer parameters using tunable diode laser absorption spectroscopy (TDLAS) in response to step-changes in pressure set-point during freeze-drying. *Journal of Pharmaceutical Sciences* **2009**, *98*, 1136-1154.

28 Milton, N.; Pikal, M.J.; Roy, M.L.; Nail, S.L. Evaluation of manometric temperature measurement as a method of monitoring product temperature during lyophilisation. *PDA Journal of Pharmaceutical Science and Technology* **1997**, *5*, 7-16.

29 Liapis, A. I.; Sadikoglu, H. Dynamic pressure rise in the drying chamber as a remote sensing method for monitoring the temperature of the product during the primary drying stage of freeze-drying. *Drying Technology* **1998**, *16*, 1153-1171.

30 Chouvinc, P.; Vessot, S.; Andrieu, J.; Vacus, P. Optimization of the freeze-drying cycle: a new model for pressure rise analysis. *Drying Technology* **2004**, *22*, 1577-1601.

31 Velardi, S.A.; Rasetto, V.; Barresi, A.A. Dynamic Parameters Estimation Method: advanced Manometric Temperature Measurement approach for freeze-drying monitoring of pharmaceutical. *Industrial Engineering Chemistry Research* **2008**, *47*, 8445-8457.

32 Fissore, D.; Pisano, R.; Barresi, A.A. On the methods based on the Pressure Rise Test for monitoring a freeze-drying process. *Drying Technology* **2011**, *29*, 73-90.

33 Pisano, R., Fissore, D., Barresi, A.A. Innovation in monitoring food freeze-drying. *Drying Technology* **2011**, *29*, 1920-1931.

34 Vallan A. A Measurement system for lyophilization process monitoring. *Proceedings of Instrumentation and measurement technology conference - IMTC 2007, Warsaw, Poland, May 1-3, 2007*.

35 Corbellini, S.; Parvis, M., Vallan, A. In-process temperature mapping system for industrial freeze dryers. *IEEE Transactions on Instrumentation and Measurement* **2010**, *59*, 1134-1140.

36 Rambhatla, S., Ramot, R., Bhugra, C., Pikal, M.J. Heat and mass transfer scale-up issues during freeze drying: II. Control and characterization of the degree of supercooling. *AAPS PharmSciTech* **2004**, *5*, Article 58.

37 Fissore, D.; Pisano, R.; Barresi, A.A. A model-based framework to get quality-by-design in freeze-drying of pharmaceuticals. In *Proceedings of Freeze Drying of Pharmaceuticals and Biologicals Conference, Garmisch-Partenkirchen, September 28 -*

October 1, 2010, 460-493.

38 Barresi, A.A.; Pisano, R.; Fissore, D.; Rasetto, V.; Velardi, S.A.; Vallan, A.; Parvis, M.; Galan, M. Monitoring of the primary drying of a lyophilization process in vials. *Chemical Engineering and Processing* **2009**, *48*, 408-423.

39 Patel, S. M., Doen, T., Pikal, M. J. Determination of end point of primary drying in freeze-drying process control. *AAPS PharmSciTech* **2010**, *11*, 73–84.

40 Barresi, A.A.; Velardi, S.A.; Pisano, R.; Rasetto, V.; Vallan, A.; Galan, M. In-line control of the lyophilization process. A gentle PAT approach using software sensors. *International Journal of Refrigeration* **2009**, *32*, 1003-1014.

41 Velardi, S.A.; Hammouri, H.; Barresi, A.A. In-line monitoring of the primary drying phase of the freeze-drying process in vial by means of a Kalman filter based observer. *Chemical Engineering Research & Design* **2009**, *87*, 1409-1019.

42 Velardi, S.A.; Hammouri, H.; Barresi, A.A. Development of a High Gain observer for in-line monitoring of sublimation in vial freeze-drying. *Drying Technology* **2010**, *28*, 256-268.

43 Bosca, S.; Fissore, D. Design and validation of an innovative soft-sensor for pharmaceuticals freeze-drying monitoring. *Chemical Engineering Science* **2011**, *66*, 5127-5136.

44 Barresi, A.A.; Pisano, R.; Rasetto, V.; Fissore, D.; Marchisio, D.L. Model-based monitoring and control of industrial freeze-drying processes: effect of batch non-uniformity. *Drying Technology* **2010**, *28*, 577-590.

List of Tables

Table 1. Parameters required to calculate the value of K_v vs. P_c for edge (V_1) and central (V_4) vials using eq. (3).

Table 2. Parameters required to calculate the value of R_p vs L_{dried} for a 5% w/w solution of sucrose and of mannitol.

List of Figures

Figure 1. Comparison between the value of R_p vs. L_{dried} measured by Lyobalance (solid line), estimated by the pressure rise test technique (symbol), and the value calculated using eq. (5) (dashed line).

Figure 2. Example of design space for two different formulations: (left graphs) 5% w/w sucrose and (right graphs) 5% w/w mannitol. The dashed line identifies the limit operating conditions nearby the endpoint of the drying, while the symbol (●) corresponds to a proper combination of operating conditions: (#1) $T_{\text{fluid}} = 255$ K and $P_c = 5$ Pa; (#2) $T_{\text{fluid}} = 252$ K and $P_c = 5$ Pa. Isoflux curves (in $\text{kg h}^{-1}\text{m}^{-2}$) are also shown.

Figure 3. Example of freeze-drying cycles carried out using the processing conditions defined via off-line optimization for (left-side graphs) 5% w/w sucrose and (right-side graphs) 5% w/w mannitol. Evolution of: (graph a) T_{fluid} and P_c ; (graph b) Pirani-Baratron pressure ratio (solid line) and J_w as estimated by the PRT technique (symbol); (graph c) T_B as measured by thermocouples (dashed line) or estimated by PRT technique (symbol). The vertical line evidences the completion of ice sublimation as detected by the pressure ratio.

Figure 4. Design space for 5% mannitol as calculated at various values of L_{dried}/L : (graph a) 1%; (graph b) 23%; (graph c) 55% and (graph d) 99%. The optimal operating conditions, and the margin of safety on T_{fluid} (vertical arrowed line), are displayed in case of a multi (left-side graphs) and single-step recipe (right-side graphs). The symbol (●) corresponds to $P_c = 5$ Pa and a specific value of fluid temperature: (#1) $T_{\text{fluid}} = 261$ K; (#2) $T_{\text{fluid}} = 252$ K; (#3) $T_{\text{fluid}} = 249$ K; (#4) $T_{\text{fluid}} = 248$ K. The and $P_c = 5$ Pa.

Figure 5. Design space for 5% w/w sucrose ($T_{\text{max}} = 240$ K) and 5% w/w mannitol ($T_{\text{max}} = 248$ K) as calculated at $L_{\text{dried}}/L = 99\%$, and considering a different value of target temperature ($T_{\text{target}} = T_{\text{max}} - \chi_{T_B}$): (solid line) $\chi_{T_B} = 0$ K; (dashed line) $\chi_{T_B} = 1$ K; (dotted line) $\chi_{T_B} = 2$ K and (dash-dotted line) $\chi_{T_B} = 3$ K.

Figure 6. Example of freeze-drying cycle carried out using a 5% w/w sucrose solution, and the model predictive control to manipulate (left-side graphs) only T_{fluid} and (right-side graphs) both T_{fluid} and P_c . Evolution of: (graph a) T_{fluid} and P_c ; (graph b) Pirani-Baratron pressure ratio (solid line) and J_w as estimated by the PRT technique (symbol); (graph c) T_B as measured by

thermocouples (dashed line) or estimated by PRT technique (symbol). The vertical line evidences the completion of ice sublimation as detected by the pressure ratio.

Figure 7. Example of freeze-drying cycle carried out using a 5% w/w mannitol solution, and the model predictive control to manipulate both T_{fluid} and P_c . Evolution of: (graph a) T_{fluid} and P_c ; (graph b) Pirani-Baratron pressure ratio (solid line) and J_w as estimated by the PRT technique (symbol); (graph c) T_B as measured by thermocouples (dashed line) or estimated by PRT technique (symbol). The vertical line evidences the completion of ice sublimation as detected by the pressure ratio.

Table 1

Parameter	Type of vial		Unit
	V₁	V₄	
$C_1 \pm \sigma_{C_1}$	21.9 ± 4.9	7.8 ± 0.5	$\text{W m}^{-2}\text{K}^{-1}$
C_2	1.04	1.04	$\text{W m}^{-2}\text{K}^{-1}\text{Pa}^{-1}$
C_3	0.04	0.04	Pa^{-1}

Table 2

Parameter	Formulation		Unit
	5% sucrose	5% mannitol	
$R_{p,0}$	2.1×10^4	1.2×10^5	m s^{-1}
P_1	1.4×10^8	1.1×10^8	s^{-1}
P_2	1.1×10^3	0.8×10^3	m^{-1}

Figure 1

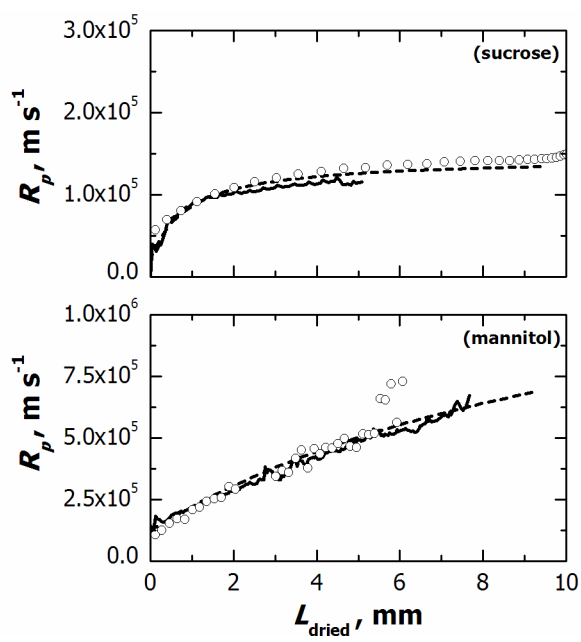


Figure 2

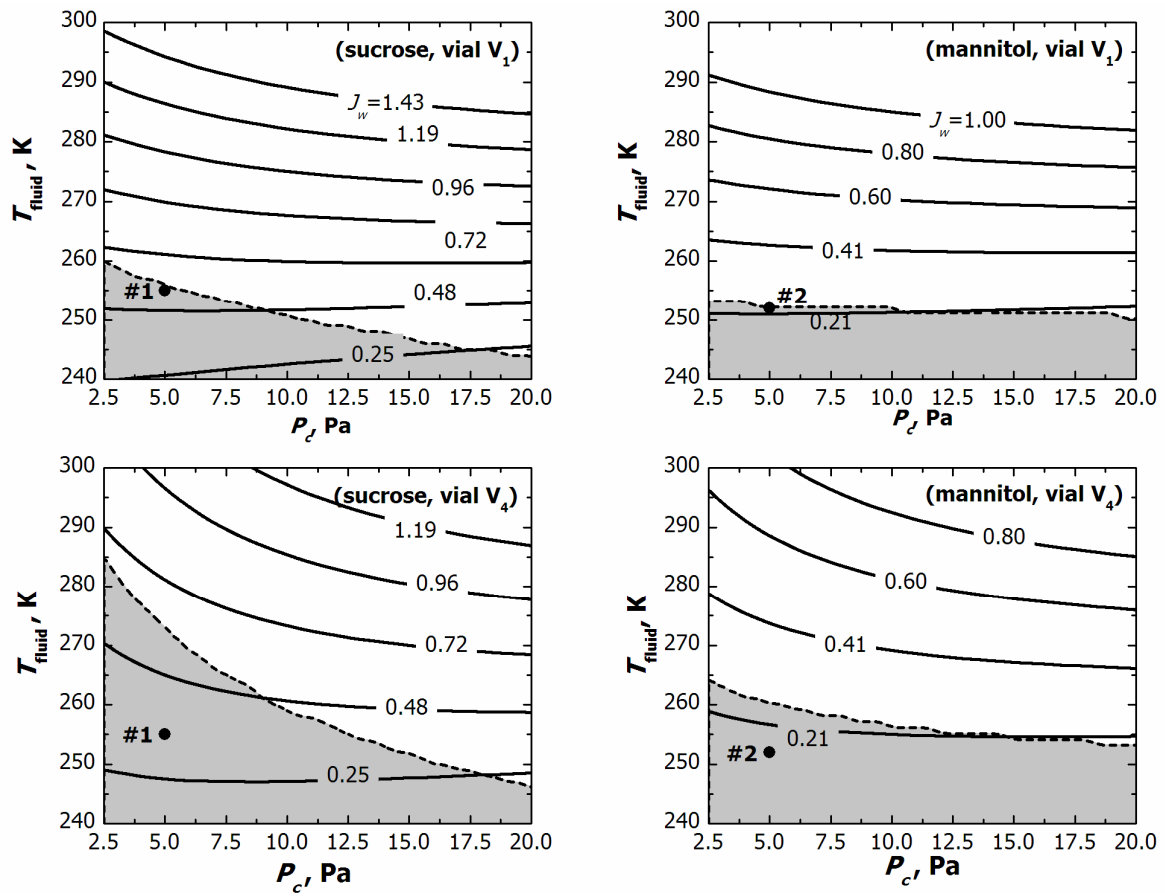


Figure 3

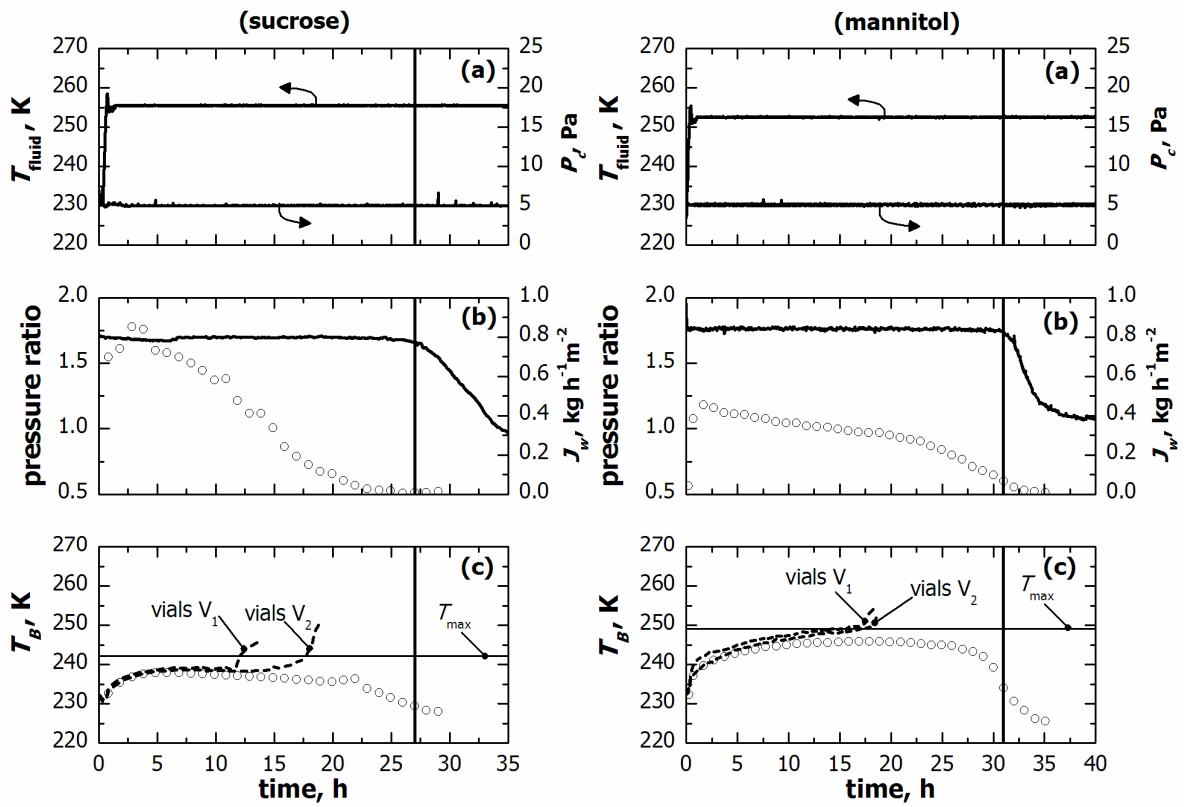


Figure 4

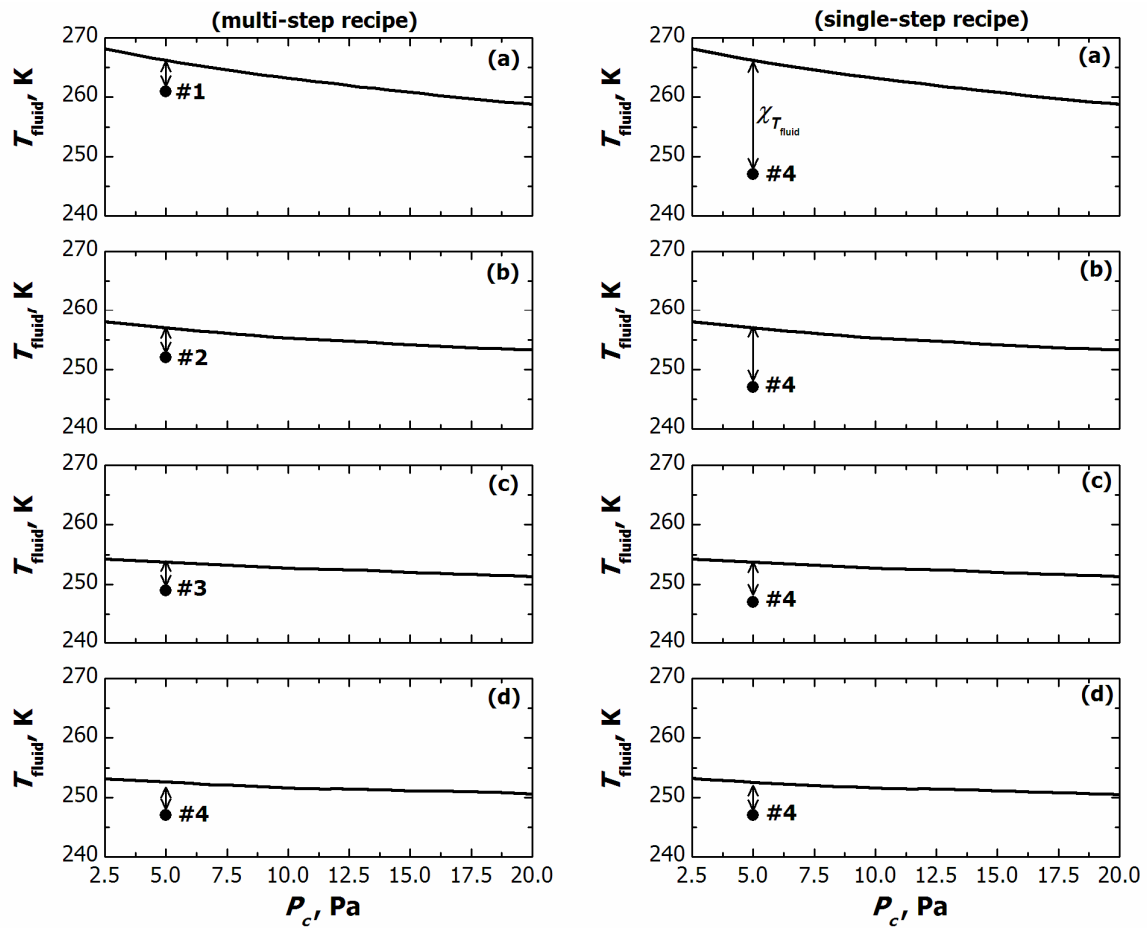


Figure 5

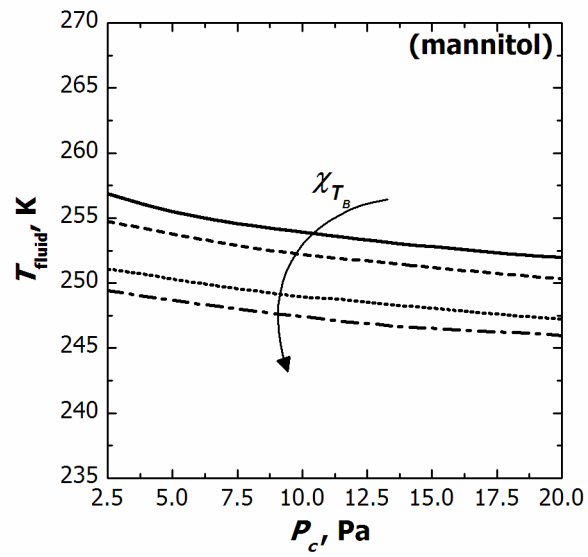
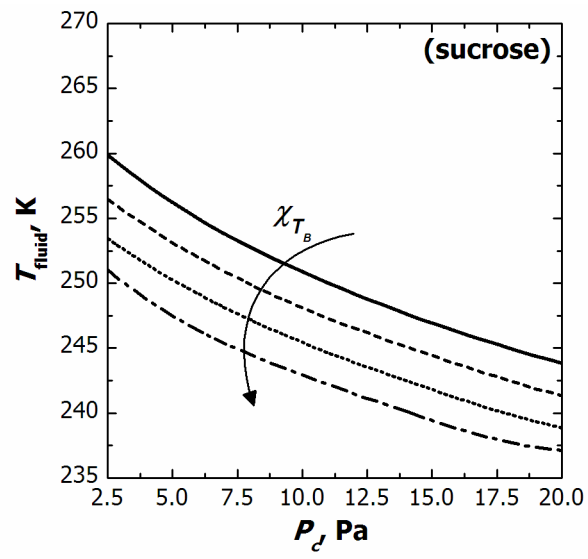


Figure 6

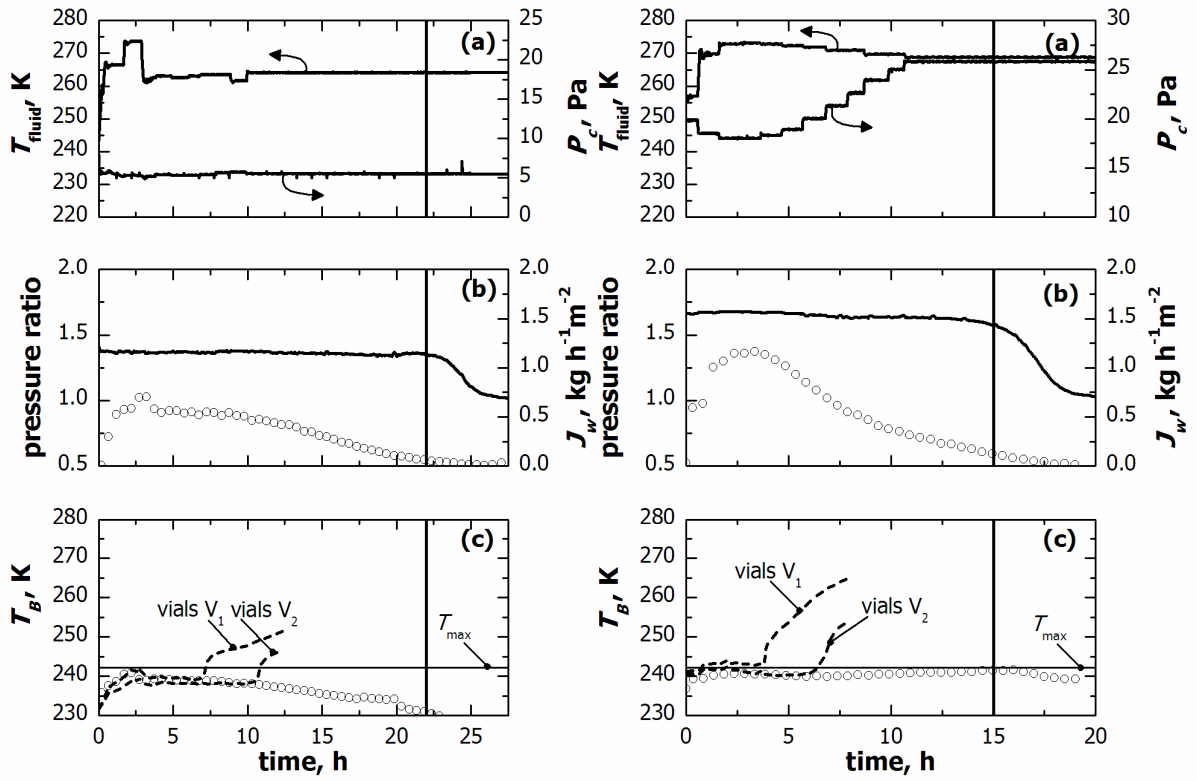


Figure 7

